Visualizing Field Lines in the FRC

Matthew Lotocki

August 2014

Overview

Magnetic fields are the key to controlling and confining plasma. The goal of this project was to develop an interactive program to visualize magnetic fields, specifically ones present in the PFRC-2 (Princeton Field Reverse Configuration 2). While exploring the shape of these fields, an interesting artifact was observed, which we called the hook. The second part of this project was to explore the hook and see how it was affected by the antenna shape.

Background

An easy way to visualize vector fields is to use a vector plot, where for each point on a grid, an arrow is drawn in the direction of the field. Although this works well with two-dimensional fields, extending it to three-dimensional fields makes it hard to see any structure or flow. The approach taken for this project was to use streamlines. Although commonly used to visualize fluid flow, streamlines can be used for any vector field, such as an electric or magnetic field. In the case of magnetic fields, streamlines are equivalent to field lines. One benefit of showing the magnetic field in the form of field lines is that small charged particles tend to follow along the field lines closely.

However, there are some challenges with streamlines. First off, in the case of magnetic field lines, one basic property is that they always close on themselves. Sometimes the field lines will extend much outside the relevant area and will be treated as infinite, but other times the field will close within the boundary of the machine, and need to be properly displayed as such. Because of this self-closing property, some streamline implementations in visualization software cannot properly handle these fields. Also, many of these visualization programs would require a three dimensional grid of points, with a vector at each point. This would require calculating the field at every point in the relevant space, even before beginning to compute streamlines. The program would then have to interpolate between points. If the grid spacing is not smaller than the integration step size, then the issue of error comes into play. This project has the advantage that there are exact known equations that govern the magnetic field, so the field can be calculated at any arbitrary point to as much precision as the computer will allow. Because of these issues, custom software was written to visualize the field lines using the exact equations. This approach saves both computational time and space.

Streamlines

As this software was built from scratch, code to calculate the streamlines needed to be written. Streamlines can be defined mathematically by the equation

$$\frac{d(\vec{\sigma}(s))}{ds} = \vec{u}(\vec{\sigma}(s)) \tag{1}$$

where $\vec{\sigma}$ is the streamline path, and $\vec{u}$ is the vector field. What this equation describes is a path that is tangent to the vector field at every point. This is also a first-order differential equation. For our implementation, it was solved using the fourth-order Runge-Kutta method. Because there is a certain amount of error in numerical integration, a closed streamline might not return to its exact starting point. To check if a field line did close, each point on the line was checked to see if it was within an arbitrarily small distance ϵ to the seed (or starting) point. We chose ϵ to be 10 times the integration step length.

There are an infinite number of streamlines for a given field, because the lines can start from anywhere. Seed points are the initial values given for the integration, and correspond to the points in the field where the lines should start, or "grow" from. Picking the right seed points is important because it affects how readable the scene is. Enough seed points are needed to show how the field is shaped, but too many and the scene becomes too crowded to read. Seed points also should be chosen in relevant areas so that the image is not crowded by unimportant regions.

Software Details

The code for this project was written in C++. For the windowing and displaying, the VTK (Visualization ToolKit) library was used. VTK was chosen because it was well-documented, provided a simple and easy way to display the field lines, and was cross platform. The project is around 2100 lines of code spread across 25 files. The code is modular, and can easily be extended upon to provide new features. It supports keyboard shortcuts to snap the camera along the three major axes, along with the ability to zoom, pan, and rotate around the field. Most aspects of the program can be changed, such as aesthetic properties like background color and streamline radius, the types of magnetic fields to display, and even internal parameters related to how the streamlines and fields are calculated. There are over 25 options that can be changed, which are put in a configuration file and given to the program at runtime.

Magnetic Fields

There are 5 different magnetic fields which can be viewed, with an option to add two fields together. The first field is the FRC (Field Reverse Configuration) field from Alan Glasser's *Theory of RMF Heating* packet. It describes the basic field present in the machine. Figure 1 shows two orthogonal cutaway planes of the field. It is composed of a radial and z component (its azimuthal component is zero). It is described by two different sets of equations, depending on if it is inside or outside of the separatrix.

Figure 1: FRC Field

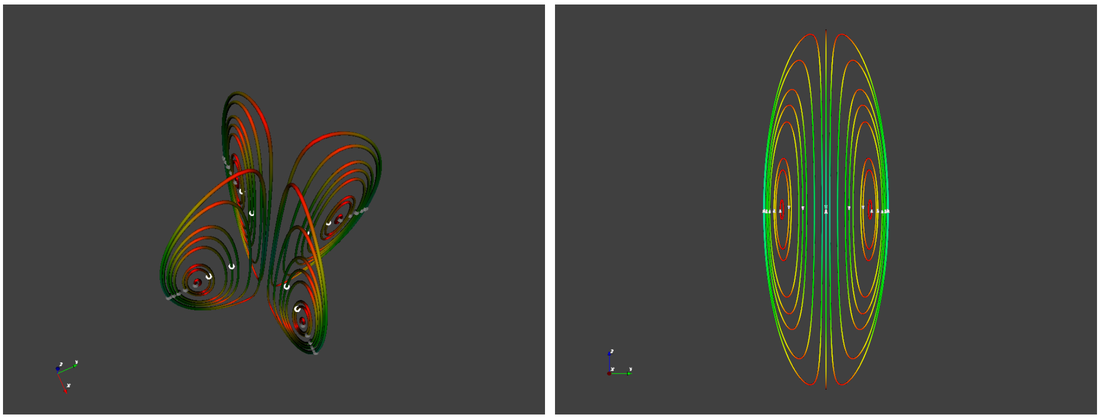

(a) Isometric view

(b) Side view

Figure 2: Antenna Configurations

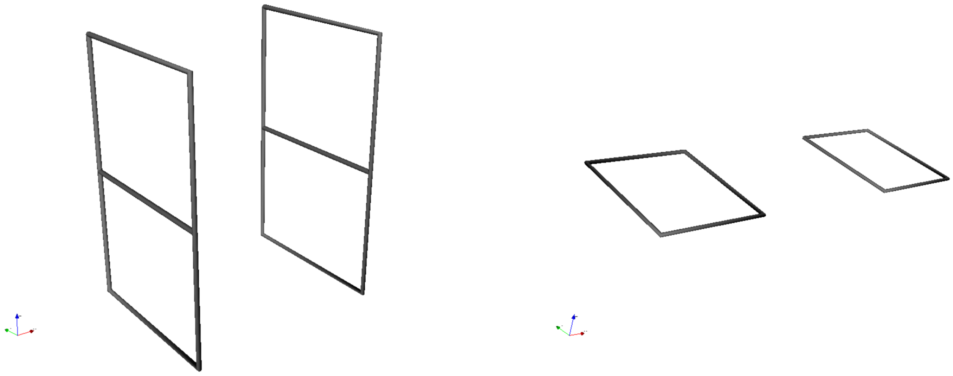

(a) Regular antenna

(b) Perpendicular antenna

The second field is the odd-parity RMF, or Rotating Magnetic Field, also from Glasser's packet. This field has a radial, azimuthal, and z component. Although not implemented in the current version of the software, the RMF field has a time dependency, where it rotates symmetrically around the z-axis.

The next three fields are the magnetic fields produce by different configurations of current carrying wire, also known as antennas. The first pair of antennas is in the shape of a window pane, as shown in Figure 2a. This is the antenna currently in use in the PFRC-2. The second antenna is a perpendicular antenna, as shown in Figure 2b. This antenna is created by folding the window pane antenna along the mid-plane so that it is perpendicular to the z-axis (but parallel to the mid-plane). Although not used in our analysis, a third antenna was implemented, which is an antenna for even parity RMF fields. It is similar to the window pane, except it is missing the middle wire. The reason for having these fields as opposed to using the RMF from Glasser is that we initially had issues implementing Glasser's RMF equations. At first, the fields were calculated using Biot-Savart's law. However, this was very slow, as it required integration along all the wires. To speed up the calculation, we used equations for the magnetic field

Figure 3: Different views of the hook

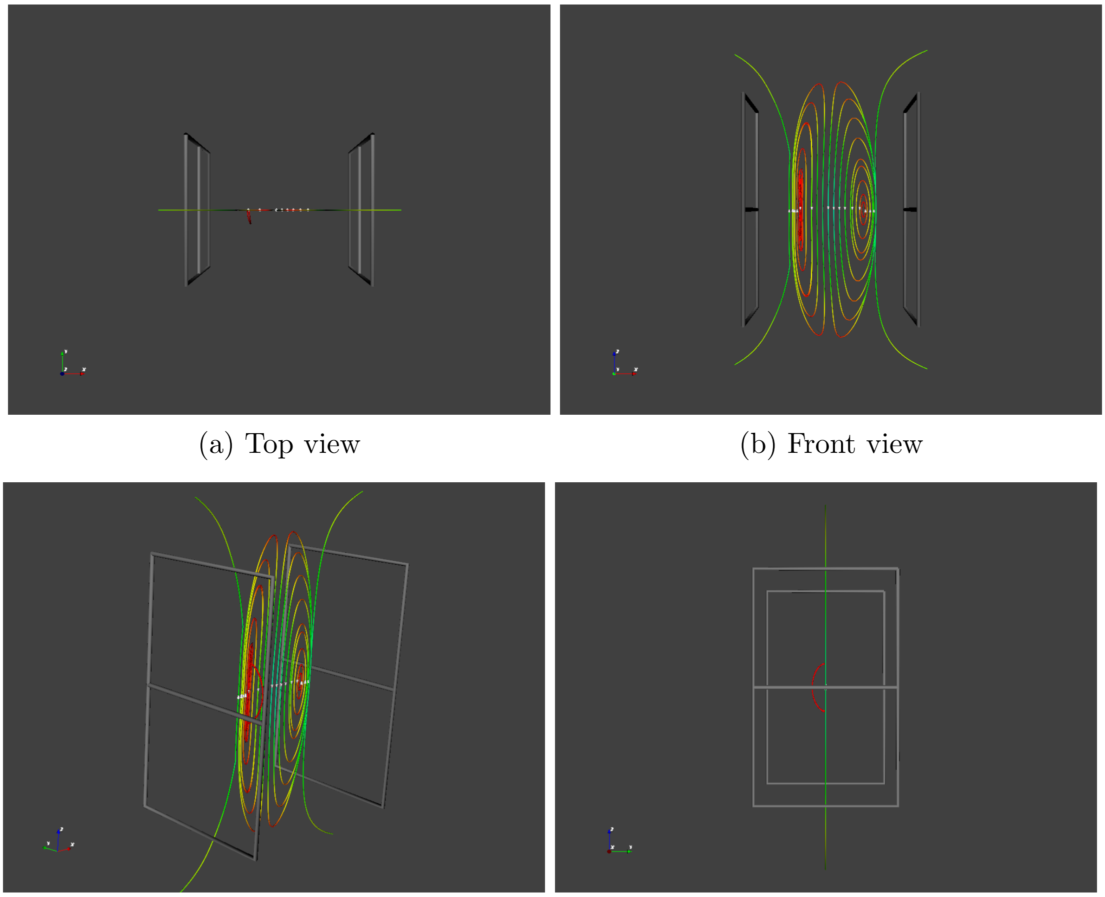

(a) Top view

(b) Front view

(c) Isometric view

(d) Side view

produced by rectangular loops. These equations meant that instead of doing multiple calculations to integrate over a wire, only one calculation was needed to be done for each rectangular loop. The Biot-Savart code was used to verify that the rectangular loop field was implemented correctly.

The Hook

The field in the FRC machine is the superposition of both an FRC field and an RMF field. While observing the field lines, a strange artifact was sometimes seen protruding perpendicular to the ϕ_0 plane. This hook is shown in Figure 3. This hook only appeared when using certain antenna configurations, and varied in size. The second part of this project was to investigate the hook. The hook was further studied to try to describe how it changes in relation to certain antenna properties. To account for where on the radial axis the hook started, its size was measured in degrees it extended around the machine. We used both the regular antenna and the perpendicular antenna to see how the choice of antenna affects the hook. The main three dimensions that were varied were the separation between the antennas, the width of the antenna, and the height of the antenna.

Figure 4: Hook sizes as a function of certain antenna parameters

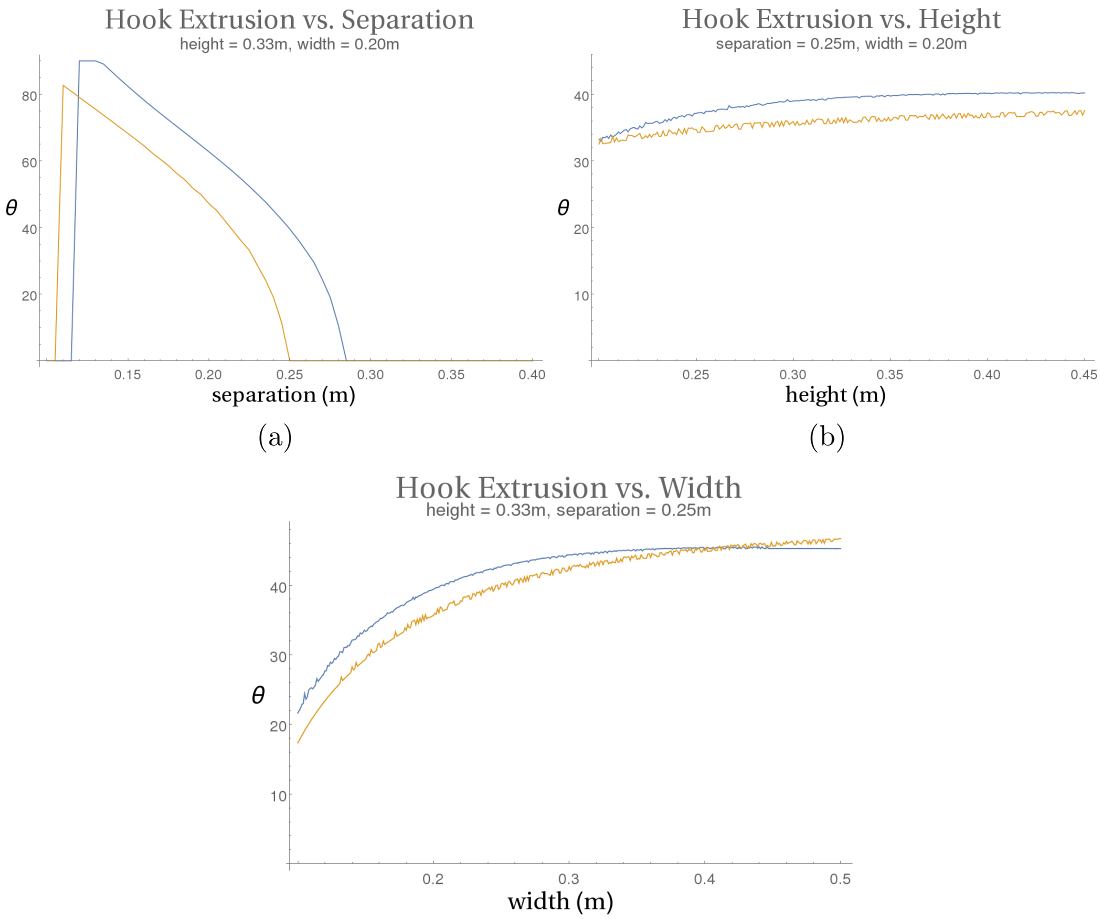

(a)

(b)

(c)

Note: Blue curves are for regular antennas, and yellow curves are for perpendicular antennas

Figure 4a shows that the size of the hook increases as the separation of the antennas decreases. This result stands for both antennas, although the curve for the perpendicular antenna is shifted to the left. It is important to note that because the radius of the separatrix used here is 0.07 meters, the values around and below its diameter of 0.14 meters have the antenna almost inside the separatrix, and produced degenerate fields.

The next variable changed was the height of the antenna, which is shown in Figure 4b. For the perpendicular antenna, this height value correlates to double the distance from the front and back wires of the antenna. The hook values do not appear to be heavily related to the height, and there is little difference between the two types of antennas used. The third variable changed was the width of the antenna, as shown in Figure 4c. The graph shows a positive correlation between the two, however it seems that the hook levels off after the antenna gets to a certain width. The hook from the perpendicular antenna is also almost identical to that of the regular antenna.

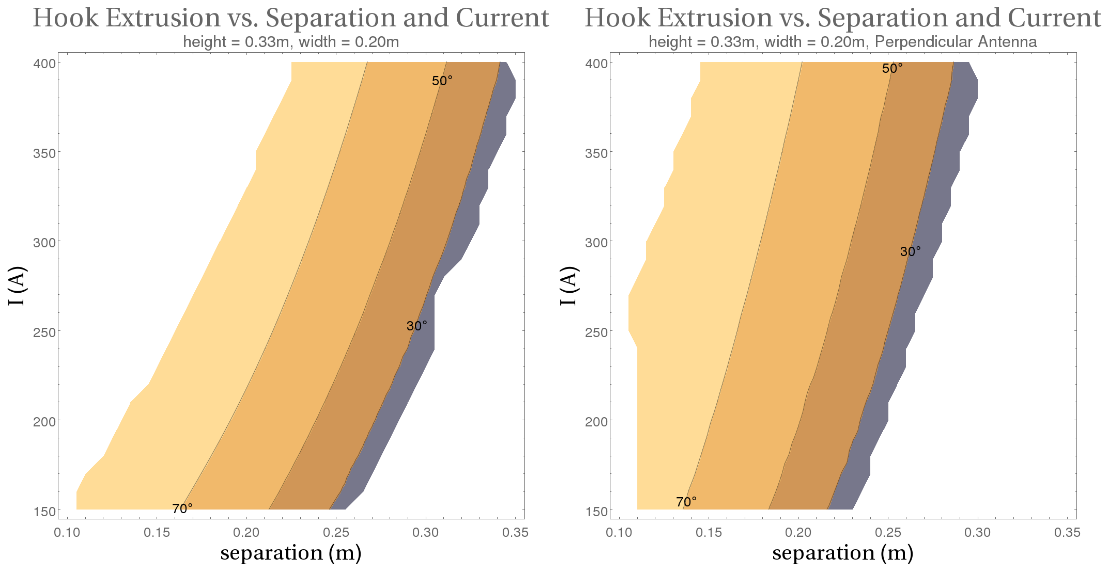

(a) Contour with regular antenna (b) Contour with perpendicular antenna

Figure 5: Contour of hook size as a function of separation and current

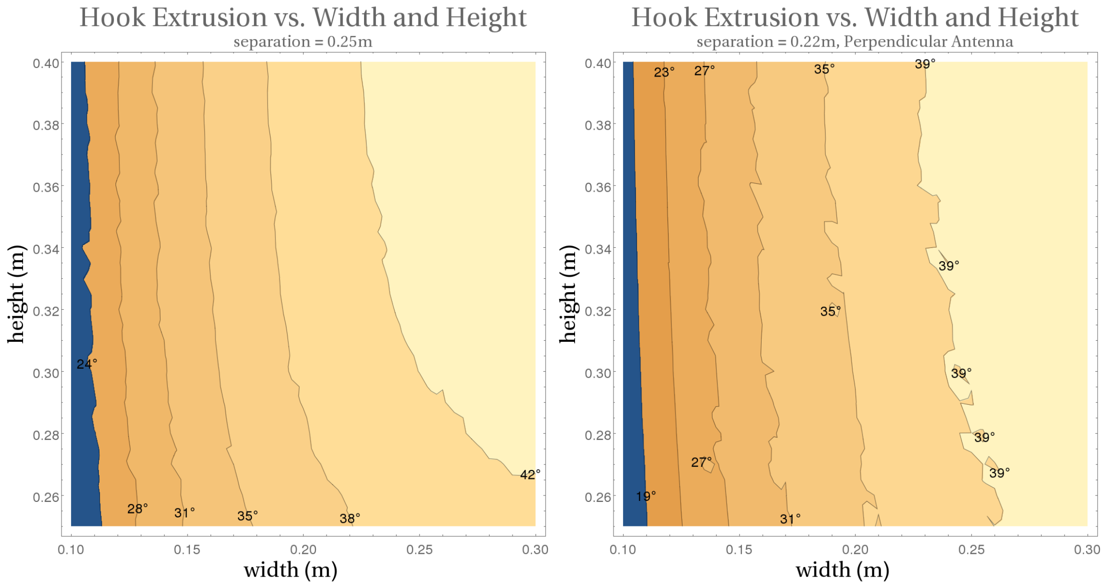

(a) Contour with regular antenna (b) Contour with perpendicular antenna

Figure 6: Contour of hook size as a function of height and width

For further analysis, we compared the hook extrusion to both the separation of antennas and the current running through the antennas. Using a contour plot (showing values only above 10 degrees), Figure 5a shows that the hook seems to be almost linearly related to both the separation and the current. Another linear relationship was seen with the perpendicular antenna in Figure 5b, although with a different slope. A similar technique was applied to width and height, to see how the specific shape of the antenna affects the hook. The graph in Figure 6a shows that for low widths, the hook does not depend much on the height, which agrees with the result we derived from Figure 4b